

## ***T-P* phase diagram for $\beta$ -(ET) $_2$ I $_3$**

V. B. Ginodman, A. V. Gudenko, P. A. Kononovich,<sup>1)</sup> V. N. Laukhin,<sup>2)</sup> and I. F. Shchegolev<sup>1)</sup>

*P. N. Lebedev Physics Institute, USSR Academy of Sciences*

(Submitted 13 November 1987)

*Zh. Eksp. Teor. Fiz.* **94**, 333–339 (May 1988)

The *T-P* diagram of  $\beta$ -(BEDT-TTF) $_2$ I $_3$  is investigated. The phase transition is determined from the jumps on the plots  $R(P)$ ,  $R(T)$ , and  $dR/dT$  of the electric conductivity. The phase-transition lines are drawn and the region of the phase diagram near the point of their intersection is investigated in detail. The phase-stability regions are determined.

### **INTRODUCTION**

It has been established by now that the quasi-two-dimensional organic metal  $\beta$ -(ET) $_2$ I $_3$  exists at low temperatures in the form of two phases: the  $\beta_L$  phase with superconducting transition temperature  $T_c = 1.5$  K, and the  $\beta_H$  phase with  $T_c = 7$ –8 K. A large number of experimental data were obtained, describing the conditions of formation of these phases, their mutual transformation, and the structural differences between them. It nevertheless remains unclear why the  $\beta_L$  and  $\beta_H$  phases, with the same chemical composition and close in their crystal structure, have superconducting transition temperatures that differ by five times.

The pure  $\beta_H$  phase under a pressure of  $\sim 1$  kbar was obtained in Refs. 1 and 2. When a  $\beta$ -(ET) $_2$ I $_3$  sample was cooled under pressure, an abrupt and complete superconducting transition was observed at  $T_c = 7$  to 8 K. Production of the  $\beta_H$  phase at normal pressure was reported in Refs. 3 and 4. The  $\beta_H$  phase was obtained by applying a small hydrostatic pressure ( $P \sim 0.5$  kbar) on a  $\beta$ -(ET) $_2$ I $_3$  crystal at room temperature, cooling under pressure, and dumping the pressure to normal at a temperature  $T \sim 100$  K. The metastable character of the  $\beta_H$  phase at low temperatures was emphasized: the  $\beta_H$  phase was preserved at normal pressure until the sample temperature reached 125–150 K (Refs. 3 and 5).

A direct determination of the  $\beta_L \leftrightarrow \beta_H$  transition from the resistance jumps was described in Refs. 6 and 7. The measurements of Ref. 6 made it possible to investigate the features of the transition between the phases, to determine the stability regions of the phases at various temperatures and pressures, and to establish the possible form of the *T-P* phase diagram.

It should be noted that under normal conditions the  $\beta$ -(ET) $_2$ I $_3$  crystals are characterized by the presence of internal disorder due to the random orientation of one of the two pairs of terminal ethylene groups of the (ET) molecules.<sup>8</sup> When the temperature is lowered at normal pressure, a phase transition takes place in  $\beta$ -(ET) $_2$ I $_3$  in the region of  $\sim 200$  K, due to the appearance of an incommensurate superstructure.<sup>9–11</sup> At  $T = 300$  K and  $P = 9.5$  kbar, on the other hand, there is neither superstructure nor disorder in the ethylene groups.<sup>12</sup> In an analysis of the *T-P* diagram proposed by us for  $\beta$ -(ET) $_2$ I $_3$  (Ref. 6) it was suggested that the singular point  $T \approx 150$  K and  $P \approx 420$  bar is either a point where the order of the transition is changed (i.e., a tricritical point), or a triple point of intersection of the lines corresponding to a superstructural transition and to ordering of

the ethylene groups. Finally, in Ref. 13 the phase diagram of  $\beta$ -(ET) $_2$ I $_3$  was investigated by the differential-thermoanalysis (DTA) method. This method made it possible to draw the second-order phase transition line predicted in Ref. 6, which intersected the hysteresis lines of the first-order phase transitions in a singular point with coordinates  $T_c = 150$  K and  $P_c = 350$  bar. The stability regions obtained in that reference for the  $\beta_L$  and  $\beta_H$  phases turned out to be quite close to the results of our investigations of the phase diagram obtained from the resistance jumps. Nonetheless, there are also some differences, which are most substantial in the region of the singular point.

We report here further investigations of the *T-P* phase diagram obtained by identifying the phase transitions by the jumps on the  $R(T)$ ,  $R(P)$ , and  $d(RT)/dT$  plots: we drew the line of superstructural second-order phase transitions (using the jumps of the derivatives  $dR(T)/dT$ ), investigated in detail the region of the diagram near the singular points, and compared the results with data by others (Refs. 10 and 13).

### **EXPERIMENT**

The electric resistance of  $\beta$ -(ET) $_2$ I $_3$  single crystals was measured as a function of temperature and pressure. Several crystals of the same composition, with characteristic dimensions  $2 \times 0.3 \times 0.05$  mm and resistance ratio  $R_{300}/R_{4.2} \approx 500$  (for the  $\beta_L$  phase), were measured. The samples were placed together with a thermometer in a cell in which a uniform pressure was produced by compression of helium gas. The pressure was continuously monitored and could be maintained constant or varied at will by cooling down to the helium freezing point.

The resistance was measured by a dc four-point method along the long crystal axis which was located in a the highly-conducting (a, b) crystallographic plane. It was necessary to forgo the use of conducting paste to secure the contacts, since the strains and stresses in the contact region produced on the  $R(T)$  and  $R(P)$  curves many parasitic nonreproducible jumps. The resistance was measured using clamped contacts. The mounting of the contacts is illustrated in Fig. 1. Sample 1, on which gold strips were sprayed, was clamped by four platinum wires 2 of 20  $\mu$ m diameter to a convex copper plate 4. This plate, covered with polymerized BF-2 adhesive, was secured to a resin-bonded paper-laminate base 5. Tension in the platinum wire was produced by metallic flat springs 3 and could be regulated for each wire separately. The contact resistance did not exceed several ohm. The

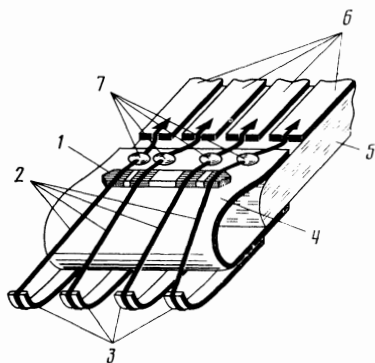


FIG. 1. Mounting of sample: 1—sample with sprayed gold contacts, 2— $20\ \mu\text{m}$  diam platinum wires, 3—metallic flat springs to tense the platinum wires, 4—copper plate (electrically insulated from sample), 5—laminate base, 6—contact plates, 7—points of attachment of platinum wires.

platinum wire were secured with droplets of glue 7 and then soldered to the copper contact plate 6. The phase state of the sample ( $\beta_L$  or  $\beta_H$ ) at a given point of the  $T$ - $P$  diagram was monitored when necessary by measuring the superconducting-transition temperature at normal pressure. To this end, the cooling and pressure reduction were effected in a manner that produced no singularities (jumps or kinks) on the  $R(T)$  and  $R(P)$  curves.

### EXPERIMENTAL RESULTS

Figure 2 shows the  $T$ - $P$  phase diagram of  $\beta$ -(ET) $_2$ I $_3$  drawn through the phase transition points ( $T$ ,  $P$ ) determined from the resistance jumps on the  $R(T)$  or  $R(P)$  plots, and also from the jumps on the plot of the derivative  $dR/dT$  vs temperature. The transitions corresponding to line  $a$  were determined from the jump on the plot of the derivative  $dR/dT$  vs temperature. Examples of such jumps at different pressures are shown in Fig. 3. At normal pressure a derivative jump is observed at  $T_A = 180 \pm 1$  K (point  $A$  of Fig. 2). With increase of pressure, the derivative-jump temperature decreases to  $T = (163 \pm 2)$  K at  $P = 425 \pm 5$  bar. Note that, within the experimental accuracy, we observed no hysteresis in the position of the jump on the plot of  $dR/dT$  vs  $T$ . This gives grounds for assuming that the transitions corresponding to line  $a$  are of second order. At pressures  $P > 430$  bar, no singularities were observed on the plots of  $dR/dT$  vs  $T$  (curves 8 and 9 of Fig. 3).

Figure 4 shows examples of  $R(T)$ - and  $R(P)$ -plot resistance jumps used to draw the lines  $b$  and  $c$  on the phase

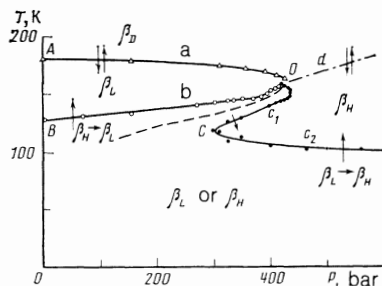


FIG. 2.  $T$ - $P$  phase diagram of  $\beta$ -(ET) $_2$ I $_3$ . Line  $a$ —line of second-order phase equilibrium between the  $\beta_D$  and  $\beta_H$  states. Lines  $b$  and  $c$ —stability limits of the  $\beta_H$  and  $\beta_L$  phases, respectively,  $d$ —hypothetical line of the  $\beta_D \leftrightarrow \beta_H$  transition (see the text).

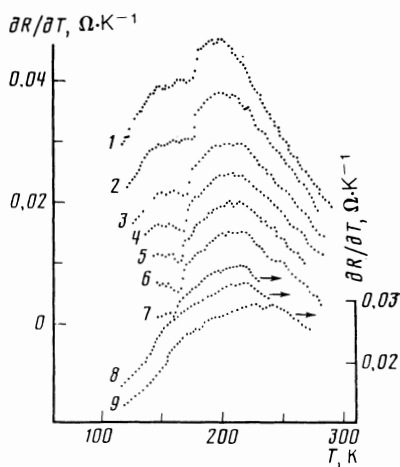


FIG. 3. Temperature dependences of the derivative  $\partial R/\partial T$  for different pressures: 1— $P = 1$  bar, 2—155 bar, 3—310 bar, 4—355 bar, 5—390 bar, 6—410 bar, 7—425 bar, 8—490 bar, 9—800 bar (the left-hand scale corresponds to curve 1, curves 2–6 are shifted downward, and curves 7–9 correspond to the right-hand scale). The jump of the derivative is due to a superstructural transition. Line  $a$  of this transition was drawn in accordance with the positions of the points of this transition.

diagram (see Fig. 2). This diagram consists of two sections,  $c_1$  and  $c_2$ . Line  $b$  is drawn using the positions of the points of the  $\beta_H \rightarrow \beta_L$  transitions accompanying heating (curves 1 and 2 on Fig. 4a) or relaxation (curves 1–4 on Fig. 4b) of a sample left in the  $\beta_H$  phase at low temperature in a preliminary  $T$ - $P$  cycle. The same curves, but obtained by cooling (loading) are observed also the reverse transitions  $\beta_L \rightarrow \beta_H$ , corresponding to the section  $c_1$  on the phase diagram. Section  $c_2$  is drawn through the points of the  $\beta_L \rightarrow \beta_H$  transition resulting from heating the  $\beta_L$  phase after compressing the sample at low temperature.

It is clear thus that the  $\beta_L \leftrightarrow \beta_H$  transition is subject to a clearly pronounced hysteresis and is of first order. This is also attested to by the character of the resistance jumps themselves, which are timed to occur at constant temperatures or pressures. We call attention to the phase-diagram region near the point  $O$  between lines  $b$  and  $c_1$ . At  $T = 150$  K and  $P = 430$  bar, the line  $c_1$  rotates smoothly and the sign of the derivative  $dP/dT$  reversed. In this region of the phase diagram, the sample can be in either the  $\beta_L$  or the  $\beta_H$  phase. The  $\beta_L$  state can be obtained in this region only by loading a sample that is already in the  $\beta_L$  phase. Corresponding to this process are the vertical lines joining the curves 2, 3, and 4 on Fig. 4a. The  $\beta_L \rightarrow \beta_H$  transition (curves 3 and 4 of Fig. 4a) occur when the sample is either heated or cooled. Following the  $\beta_L \rightarrow \beta_H$  transitions, the resistance plot becomes reversible and corresponds to the dependence of the resistance of the sample in the  $\beta_H$  state, and no reverse  $\beta_H \rightarrow \beta_L$  transition takes place.

As the point  $O$  with coordinates  $T_0 = 160 \pm 2$  K and  $P_0 = 420 \pm 5$  bar is approached, the hysteresis is gradually decreased, and at the point  $O$  itself the hysteresis and the resistance jumps vanish (curves 5 and 6 of Fig. 4b). Note that the position of the point  $C$  on the phase diagram can vary from sample to sample to a greater degree than the position of the point  $B$ . Thus, in our earlier study<sup>6</sup> the minimum pressure  $P_c$  at which the  $\beta_L \rightarrow \beta_H$  transition was observed was  $\sim 200$  bar. In the present study, for differently synthesized samples, the value of  $P_c$  turned out to be  $\approx 300$

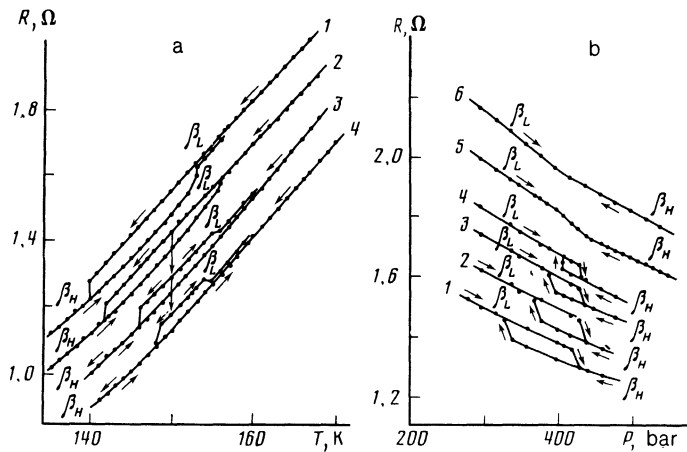


FIG. 4. Examples of transitions accompanied by a resistance jump on the  $R(T)$  (a) and  $R(P)$  (b) plots, in accordance with which the lines  $b$  and  $c$  of the phase diagrams are drawn: a) 1— $P = 400$  bar, 2—410 bar, 3—425 bar, 4—430 bar; b) 1— $T = 144$  K, 2—148 K, 3—152 K, 4—155 K, 5—160 K, 6—163 K, 7—166 K.

bar. At the same time the temperature of the  $\beta_H \rightarrow \beta_L$  transition at  $P = 1$  bar (point B on Fig. 2) hardly changes from sample to sample and is equal to  $T_B = 126$  K, in good agreement with the published data.<sup>6,7,13</sup> The equilibrium line  $\beta_H \leftrightarrow \beta_L$  should to all appearances be located closer to the hysteresis branch  $b$ . Its hypothetical form is shown on the phase diagram by a dashed line. In view of the strong hysteresis in the low-temperature region, it is impossible to identify the axis ( $T$  or  $P$ ) which the line crosses, or the phase ( $\beta_H$  or  $\beta_L$ ) that is metastable in the helium-temperature region.

## DISCUSSION

As mentioned in the Introduction, under normal conditions a feature of  $\beta$ -(ET)<sub>2</sub>I<sub>3</sub> crystals is the presence of internal disorder connected with the random orientation of the ethylene groups of the (ET) molecules.<sup>8</sup> When the temperature at atmospheric pressure is lowered, a phase transition takes place<sup>9,10,12</sup> in  $\beta$ -(ET)<sub>2</sub>I<sub>3</sub> near  $T = 200$  K, with formation of an incommensurate superstructure. An analysis in Ref. 14 indicates that this transition causes ordering of those (ET)-molecule ethylene groups which occupy randomly prior to the transition one of the two possible positions and are deflected to one or the other side of the molecule plane. After formation of the superstructure, these terminal groups are deflected to one side in one half-period of the superstructure and to the other side in the other. The phase state characterized by the presence of a superstructure is preserved down to helium temperatures, and it is precisely in this state (phase  $\beta_L$ ) that the superconducting transition with  $T_c = 1.5$  K takes place. The jump of the derivative  $dR/dT$ , observed by us at normal pressure and at  $\sim 180$  K is due to the this superstructure transition, and therefore line  $a$  of our  $T$ - $P$  diagram is the line of the irreversible hysteresis-free second-order phase transition  $\beta_D \leftrightarrow \beta_L$  (we designate by  $\beta_D$  the  $\beta$ -(ET)<sub>2</sub>I<sub>3</sub> phase with disordered ethylene groups).

In contrast to the  $\beta_L$  phase with  $T_c = 1.5$  K, the phase  $\beta_H$  with  $T_c = 8$  K features not only absence of a superstructure, but apparently also complete ordering of the ethylene groups.<sup>11</sup> This last assumption is confirmed by our earlier data,<sup>6</sup> which have shown that the residual resistance in the  $\beta_H$  state is smaller by 1.5–2 orders than the analogous value for a sample in the  $\beta_L$  state.

In accordance with our  $T$ - $P$  diagram (see Fig. 2), it is possible to land in the  $\beta_H$  state from the  $\beta_D$  state in two

ways: by circling around the point  $O$  counterclockwise or clockwise. In the first case, crossing the lines  $a$  and  $c_1$ , we observe the two phase transitions  $\beta_D \rightarrow \beta_L \rightarrow \beta_H$ , and in the second case no singularities are recorded in the  $R(T)$ ,  $R(P)$ , and  $dR/dT$  curves. The latter may be evidence that on circling around the point  $O$  clockwise the ordering of the ethylene groups, which is typical of the  $\beta_H$  state, is continuous, without a phase transition. In this case the point  $O$  on the phase diagram is tricritical (i.e., a point where the order of the transition changes). We, however, consider it more likely that  $O$  is a triple point, and by bypassing it from the right we should cross somewhere the phase-transition line. This hypothetical line is shown by the dash-dot line  $d$  in Fig. 2. The justification for drawing the line  $d$  with a positive slope ( $dT/dP > 0$ ) is that according to Ref. 12 there is neither disorder of the ethylene groups nor a superstructure in  $\beta$ -(ET)<sub>2</sub>I<sub>3</sub> samples at  $T = 300$  K and  $P = 9.5$  kbar.

The fact that on crossing the hypothetical line  $d$  we record no resistance singularities indicates that the disorder of the ethylene groups does not lead to additional carrier scattering. At the same time, the jumps we have observed in the resistance or in the derivative  $dR/dT$  for the transition  $\beta_D \rightarrow \beta_L$  or  $\beta_L \rightarrow \beta_D$  are evidence that it is precisely the onset of the superstructure which makes the additional contribution to the carrier scattering. This is apparently due to the incommensurability of the superstructure with the principal lattice, which leads to the onset of a random potential from which the carriers are additionally scattered.

The equilibrium lines  $a$  and  $d$  drawn by us (see Fig. 2) for the phase transitions  $\beta_D \leftrightarrow \beta_L$  and  $\beta_D \leftrightarrow \beta_H$  respectively, and the hysteresis branches  $b$  and  $c$  of the transition intersect thus at the triple point  $O$  with coordinates  $T_0 \approx 160$  K and  $P_0 \approx 430$  bar and break up the  $T$ - $P$  phase plane into four regions. Above the lines  $a$  and  $d$  is located the stability region of the disordered phase  $\beta_D$ . Between lines  $a$ ,  $b$  and  $c$ ,  $d$  are located the stability regions of phases  $\beta_L$  and  $\beta_H$ , respectively. Finally, lines  $b$  and  $c$  bound the metastability region in which both phase  $\beta_L$  and phase  $\beta_H$  can exist.

Note that the phase diagram obtained by us is somewhat at variance with the results of Refs. 11 and 13. The neutron-diffraction investigations of Ref. 11 have shown that the superstructure featured by the  $\beta_L$  phase was observed in a cycle in which the sample was cooled from room temperature to 20 K at a pressure  $P = 500$  bar. From our  $T$ -

$P$  diagram it is seen that when cooling in this manner we circle the point  $O$  clockwise and  $\beta$ -(ET) $_2$ I $_3$  should have no superstructure down to helium temperatures.

In the phase diagram obtained in Ref. 13 by the DTA method, the point that determines the process of obtaining the  $\beta_H$  phase at low temperature turned out to be the point of intersection of phase-transition lines, or the singular point  $O$  in our terminology. The reason is that the phase-transition line  $c$  in Ref. 13 has no section with a positive derivative  $dP/dT$  (section  $c_1$  in Fig. 2), and consequently there is likewise no point at which the derivative  $dP/dT$  reverses sign, a point which is decisive for obtaining the  $\beta_H$  phase at low temperature. The difference is possibly due to the insufficient accuracy, admitted by the authors of Ref. 13, of the measurements in the region of the singular point, which lead to a rather approximate determination of the shapes of the lines in this region, and accordingly of their intersection point.

We conclude by advancing certain assumptions that explain the substantial difference between the superconducting temperatures of the  $\beta_L$  and  $\beta_H$  phases. Note that according to NMR data<sup>14</sup> the onset of a superstructure does not lead to a substantial difference between the densities of the electronic states. If the strong difference between the values of  $T_c$  of phases  $\beta_L$  and  $\beta_H$  is due only to the presence or absence of disorder, the disorder of the  $\beta_L$  phase is so strong that this phase is close to the Anderson transition, which is unlikely, or we are dealing with a triplet superconductivity, since the presence of weak disorder does not influence the value of  $T_c$  in the case of singlet pairing. In addition, the difference in  $T_c$  can be due to a change of the phonon spectrum of  $\beta$ -(ET) $_2$ I $_3$  as a result of formation of a superstructure.

In conclusion, the authors are deeply grateful to L. N. Bulaevskii and to L. N. Zherikhina for interest in the work and for a helpful discussion.

<sup>1</sup>Institute of Solid State Physics, USSR Academy of Sciences, Chernogolovka.

<sup>2</sup>Division of Institute of Chemical Physics, USSR Academy of Sciences, Chernogolovka.

<sup>1</sup>V. N. Laukhin, E. E. Kostyuchenko, Yu. V. Sushko, *et al.*, Pis'ma Zh. Eksp. Teor. Fiz. **41**, 68 (1985) [JETP Lett. **41**, 81 (1985)].

<sup>2</sup>K. Murata, M. Tokumoto, H. Anzai, *et al.*, J. Phys. Soc. Jpn. **54**, 1236 (1985). K. Murata, M. Tokumoto, and H. Anzai, *ibid.* p. 2084.

<sup>3</sup>V. B. Goodman, A. V. Gudenko, I. I. Zasavitskii, and E. B. Yagubskii, Pis'ma Zh. Eksp. Teor. Fiz. **42**, 384 (1985) [JETP Lett. **42**, 472 (1985)].

<sup>4</sup>F. Creuzet, G. Creuzet, D. Jerome, *et al.*, J. Phys. Lett. **46**, 1079 (1985).

<sup>5</sup>F. Creuzet, D. Jerome, D. Sohweitzek, and H. Keller, Europhys. Lett. **1**, 461 (1986).

<sup>6</sup>V. B. Ginodman, A. V. Gudenko, P. A. Kononovich, *et al.*, Pis'ma Zh. Eksp. Teor. Fiz. **44**, 523 (1986) [JETP Lett. **44**, 673 (1986)].

<sup>7</sup>B. Hamzic, B. Creuzet, and C. Lenoir, Europhys. Lett. **3**, 373 (1987).

<sup>8</sup>R. P. Shibaev, V. I. Kaminskii, T. I. Prokhorova, and E. B. Yagubskii, Pis'ma Zh. Eksp. Teor. Fiz. **39**, 15 (1984) [JETP Lett. **39**, 17 (1984)].

<sup>9</sup>P. Leung, T. Emge, M. Beno, *et al.*, J. Am. Chem. Soc. **106**, 7644 (1984).

<sup>10</sup>T. Emge, P. Leung, M. Beno, *et al.*, Phys. Rev. **B30**, 6760 (1984).

<sup>11</sup>A. Schultz, M. Beno, H. Wang, and J. Williams, *ibid.* **B33**, 7823 (1986).

<sup>12</sup>V. N. Molchanov, R. P. Shibaeva, V. I. Kaminskii, *et al.*, Dokl. Akad. Nauk SSSR **286**, 637 (1986) [Sov. Phys. Doklady **31**, 6 (1986)].

<sup>13</sup>W. Kang, G. Creuzet, D. Jerome, and C. Lenoir, J. de Phys. **48**, 1035 (1987).

<sup>14</sup>P. Leung, T. Emge, M. Beno, *et al.*, J. Am. Chem. Soc. **107**, 6184 (1985).

Translated by J. G. Adashko